1985

NASA/ASEE SUMMER FACULTY RESEARCH FELLOWSHIP PROGRAM

MARSHALL SPACE FLIGHT CENTER

THE UNIVERSITY OF ALABAMA

ANALYTICAL DETERMINATION OF SPACE STATION RESPONSE TO CREW MOTION AND DESIGN OF SUSPENSION SYSTEM FOR MICROGRAVITY EXPERIMENTS

Prepared By:	Frank C. Liu, Ph.D., PE
Academic Rank:	Professor
University and Department:	The University of Alabama in Huntsville Department of Mechanical Engineering
NASA/MSFC	
Division:	Mechanical
Branch:	Mechanical System Development
MSFC Counterpart:	Harold Smyly
Date:	August 1, 1985
Contract No.:	NGT-01-008-021 The University of Alabama in Huntsville

ANALYTICAL DETERMINATION OF SPACE STATION RESPONSE TO CREW MOTION AND DESIGN OF SUSPENSION SYSTEM FOR MICROGRAVITY EXPERIMENTS

by

Frank C. Liu

Professor of Mechanical Engineering
The University of Alabama in Huntsville
Huntsville, Alabama

ABSTRACT

The objective of this investigation is to make analytical determination of the acceleration produced by crew motion in an orbiting space station and define design parameters for the suspension system of microgravity experiments. A simple structural model for simulation of the IOC space station is proposed. Mathematical formulation of this model provides the engineers a simple and direct tool for designing an effective suspension system.

ACKNOWLEDGMENT

It has been an exciting experience for me to work on this interesting project. I am grateful to Mr. Doug Lamb, Chief of Mechanical Division, Structures and Propulsion Laboratory, and his staff Mr. Charles Cornelius, Mr. Harold Smyly, and Mr. Charles Miller for giving me an enjoyable summer to carry out this investigation. I express appreciation to Mr. Mike Moore, my office mate, for making all the computer graphs. Special thanks are due to Ms. Margarete Landers for typing this report.

TABLE OF CONTENTS

LIST OF FIGURES

LIST OF TABLES

1. Introduction

Some microgravity experiments to be performed on the IOC space station require an environment in which the acceleration level must be below 10^{-5} g. Among the various sources of disturbances, crew motion is the severe one which can produce acceleration to a magnitude of 10^{-4} g. The objectives of this investigation are to define design characteristics for the suspension system and to find effective means for isolation of the experiment packages from disturbance. To achieve these goals, the following have been accomplished.

1. Analytical formulation of acceleration response of IOC to crew motion

Assumed modes method and modal transformation are used to obtain mathematical solution for the normal coordinates to an input function due to crew motion. Acceleration response of any point in the space station can be analytically formulated.

2. Structural modeling for IOC space station

The finite element model for IOC space station, shown in Figure 1, used by JFC [1] for vibration analysis generates a wide range and closely spaced spectrum of vibration frequencies (see Table 4.3.3.3-3, reference 1). It makes it extremely difficult for mechanical design engineers to identify a particular mode which has dominant effect on the experiment package. A simple structural model which is made of a rigid main body (extension of keel frame which supports all the massive modules), a cantilever beam (the keel frame), and a transverse cantilever beam (the solar boom) is proposed for simulation of the IOC. A complete analytical formulation for this model is made. This formulation provides the design engineers a simple and direct tool for determination of acceleration and disturbing frequencies acting on the experiment package. Computations can be carried out by using a pocket calculator. This model can be easily improved by increasing the degrees-of-freedom. A simple computer program will do this work.

3. Derivation of design characteristics for suspension system

Consider that a microgravity experiment package is supported by a spring and a mass-spring-damper vibration absorber is attached to it. The acceleration magnification factor and the ratio of acceleration response of package to acceleration input of the support is then derived. The plots of this factor versus frequency ratio (IOC to mass-spring) provide engineers design parameters of the suspension system.

4. Significant findings for effective isolation of disturbance

The microgravity laboratory is 23.3/83.2 feet from the center of mass of IOC with/without the orbiter attached. It is shown by

numerical study that the acceleration disturbance is greatly reduced when the orbiter is not present (i.e., microgravity lab is actually 59.9 feet farther away from the C.M. of IOC). This shows that the most favorable location beside the C.M. of IOC is the node of the fundamental elastic vibration mode of the IOC.

2. Analytical Formulation

2.1 Modal analysis of a structure system

A brief presentation of modal analysis of a structure is given here. Let P be the coordinate of a generic mass point P in a structure and u(P,t) be its displacement which is expressed in the form [2]

$$u(P,t) = \sum_{i=1}^{N} \psi_i(P) q_i(t) \tag{2.1}$$

where $\psi_i(P)$ is an admissible function and $q_i(t)$ is the ith generalized coordinate of a set N. The equation of motion of the structure system in matrix form is

$$[m]\ \{\ddot{q}\} + [k]\ \{q\} = \{Q\} \tag{2.2}$$

where [m], [k], and {q} are the generalized mass, stiffness, and force matrices, respectively.

The kinetic and bending strain energies of the system are formulated from the following integrals:

$$T = \tfrac{1}{2}\int_B m_P[\dot{u}(P,t)]^2\ dP = \tfrac{1}{2}\sum\int_B m_P\psi_i^{\,2}(P)dP\dot{q}_i^{\,2} \tag{2.3}$$

$$V = \tfrac{1}{2}\int_B EI[u''(P,t)]^2 dP = \tfrac{1}{2}\sum\int_B m_P[\psi_i''(P)]^2\ dPq_i^{\,2} \tag{2.4}$$

where m_P is the mass density at P and EI is the bending stiffness of the structure at P, the prime denotes partial differentiation with respect to spatial coordinates and the symbol B with the integral sign means integration over the entire body B. From the above integrals, the elements of the [m] and [k] matrices are obtained respectively,

$$m_{ij} = \frac{\partial^2 T}{\partial\dot{q}_i\partial\dot{q}_j} = \int_B m_P\psi_i(P)\psi_j(P)dP \tag{2.5}$$

$$k_{ij} = \frac{\partial^2 V}{\partial q_i \partial q_j} = \int_B EI\psi_i''(P)\psi_j''(P)dP \tag{2.6}$$

Denoting the force acting at P in the direction of u(P,t) by $f_p(t)$, then the virtual work is

$$\delta W = \int_B f_p(t)\delta u dP = \sum \int_B f_p \psi_i(P)\delta q_i dP \tag{2.7}$$

It follows that

$$Q_i = \frac{\partial W}{\partial q_i} = \int_B f_p \psi_i(P)dP \tag{2.8}$$

Next, the natural frequencies of the system are determined from the determinant

$$\left|[k] - \omega^2[m]\right| = 0 \tag{2.9}$$

and the eigenvectors (or modal columns) $\{\phi_i\}$ are the solution of the matrix equations,

$$([k] - \omega_i^2[m])\ \{\phi_i\} = \{0\} \qquad i = 1,2,\ldots,N \tag{2.10}$$

The normal coordinates $\{\eta\}$ and the generalized coordinates are related by the transformation

$$\{q\} = [\Phi]\ \{\eta\} \tag{2.11}$$

where the modal matrix

$$[\Phi] = [\{\phi_1\}, \{\phi_2\}, \ldots, \{\phi_N\}]$$

Applying Eq. (2.11) to Eq. (2.2) and making use of the property of generalized orthogonality of the eigenvector with respect to [m] and [k], the equation of motion in normal coordinates is

$$\ddot{\eta}_j + \omega_j^2\ \eta_j = N_j(t)/M_{jj} \qquad j = 1,2,\ldots,N \tag{2.12}$$

where

$$M_{jj} = \{\phi_j\}^T[m]\{\phi_j\} \tag{2.12a}$$

$$\omega_j^2 = \{\phi_j\}^T[k]\{\phi_j\}/M_{jj} \tag{2.12b}$$

$$N_j(t) = \{\phi_j\}^T\{Q\} \quad . \tag{2.12c}$$

2.2 Structure response to disturbing force

Consider that a disturbing force $f_a(t)$ is applied to the structure at P_a, from Eqs. (2.8) and (2.12c) one obtains

$$N_j(t) = \sum_{k=1} \phi_{kj}\psi_k(P_a)f_a(t) \tag{2.13}$$

where ϕ_{kj} is the kth element of the jth eigenvector. The response at point P_e in the structure, $u(P_e,t)$, can be obtained by using Eqs. (2.1), (2.11), and (2.13). It results in

$$u(P_e,t) = \sum_i \psi_i(P_e)q_i(t) = \sum_i \sum_j \psi_i(P_e)\phi_{ij}\eta_j(t)$$

$$= \sum_j \left[\left(\sum_i \phi_{ij}\psi_i(P_e)\right)\left(\sum_k \phi_{kj}\psi_k(P_a)\right)\right] \bar{\eta}_j(t)/M_{jj} \tag{2.14}$$

where $\bar{\eta}_j(t)$ denotes the solution of the differential equation,

$$\ddot{\eta}_j + \omega_j^2\eta_j = f_a(t) \qquad \text{with} \qquad \eta_j(0) = \dot{\eta}_j(0) = 0 \quad . \tag{2.15}$$

2.3 Model of crew motion and response function

The motion of an astronaut inside a space module is started by pushing one wall and motion is stopped by pushing the opposite wall. A simple mathematical model is suggested [1] as shown in Figure 2.

$$f_a(t) = \begin{cases} (f_o/t_1)t & 0 < t \leq t_1 \\ 0 & t_1 < t \leq t_{13} \\ (f_o/t_1)(t - t_{14}) & t_{13} < t \leq t_{14} \\ 0 & t_{14} < t \end{cases} \tag{2.16}$$

The magnitude of f_o is 25 lbs and t_1, t_{13}, and t_{14} are 1, 13, and 14 seconds, respectively. These notations for time will be kept through the formulation for the sake that one may wish to change their magnitudes and secondly, that the equation involved will have appropriate units (use $\sin\omega t_{13}$ rather than $\sin 13\omega$ where ω is in rad/s). The solution of equation (2.15) is readily obtained. Denoting that

$$\eta(t) = (f_o/\omega^3 t_1)U(t) \tag{2.17}$$

the dimensionless displacement function U(t) is given by

$0 < t \leq t_1$ $\quad U(t) = \omega t - \sin\omega t$ (2.17a)

$t_1 < t \leq t_{13}$ $\quad U(t) = -\sin\omega t + \sin\omega(t - t_1) + \omega t_1 \cos\omega(t - t_1)$ (2.17b)

$t_{13} < t \leq t_{14}$ $\quad U(t) = \omega(t - t_{14}) - \sin\omega t + \sin\omega(t - t_1)$
$- \sin\omega(t - t_{13}) + \omega t_1[\cos\omega(t - t_1)$
$+ \cos\omega(t - t_{13})]$ (2.17c)

$t_{14} < t$ $\quad U(t) = -\sin\omega t + \sin\omega(t - t_1) - \sin\omega(t - t_{13})$
$+ \sin\omega(t - t_{14}) + \omega t_1[\cos\omega(t - t_1)$
$+ \cos\omega(t - t_{13})]$ (2.17d)

The function U(t) is continuous and has continuous first derivative (velocity); its second derivative is only piecewise continuous. Denoting

$$\ddot{\eta}(t) = (f_o/\omega t_1)A(t) \tag{2.18}$$

and differentiating Eq. (2.17) twice, one obtains the dimensionless acceleration A(t),

$$0 < t \leq t_1 \qquad A(t) = \sin\omega t \tag{2.19a}$$

$$t_1 < t \leq t_{13} \qquad A(t) = \sin\omega t - \sin\omega(t - t_1) - \omega t_1 \cos\omega(t - t_1) \tag{2.19b}$$

$$t_{13} < t \leq t_{14} \qquad A(t) = \sin\omega t - \sin\omega(t - t_1) + \sin\omega(t - t_{13}) - \omega t_1 \left[\cos\omega(t - t_1) + \cos\omega(t - t_{13})\right] \tag{2.19c}$$

$$t_{14} < t \qquad A(t) = \sin\omega t - \sin\omega(t - t_1) + \sin\omega(t - t_{13}) - \sin\omega(t - t_{14}) - \omega t_1 \left[\cos\omega(t - t_1) + \cos\omega(t - t_{13})\right] \tag{2.19d}$$

The functions of U(t) and A(t) are plotted versus time for frequencies ranging from 0.1 to 0.4 as shown in Figures 3 and 4 respectively. Now, the displacement and acceleration response of point P_e in the space station can be expressed in the form

$$u(P_e,t) = \sum_j \left(\sum_i \phi_{ij}\psi_i(P_e) \right) \left(\sum_k \phi_{kj}\psi_k(P_a) \right) U_j(t)(f_o/\omega_j{}^3 t_1 M_{jj}) \tag{2.20a}$$

$$a(P_e,t) = \sum_j \left(\sum_i \phi_{ij}\psi_i(P_e) \right) \left(\sum_k \phi_{kj}\psi_k(P_a) \right) A_j(t)(f_o/\omega_j t_1 M_{jj}) \tag{2.20b}$$

The subscript "j" with U and A denotes that these functions are corresponding to $\omega = \omega_j$.

2.4 Modeling of IOC space station

The structure of the IOC space station may be treated as a structural system having three elements. The main body is a frame structure which supports all the massive members, the vertical and horizontal HAB modules, the vertical and horizontal LAB modules, logistic and common modules, and above all, the orbiter. Attached to the main body is a keel frame structure 296 feet in length which supports an antenna system at its other end and a transverse boom at a distance 165.5 feet from the main body. The third member of the system is a transverse boom which is a frame structure 264 feet long. Its main purpose is to carry eight solar arrays and power system radiators.

A simple structural model for the IOC proposed consists of a rigid main body which supports a cantilever beam (keel frame) and a transverse cantilever beam (solar boom) mounted on the keel. As shown in Table 1 in Appendix A, the modules, equipment, solar arrays, fuel tanks, orbiter, etc., are treated as concentrated masses. However, the rotational moments of inertia of the orbiter and solar arrays must be included in forming the mass matrix.

Motions of the IOC in X-Z and Y-Z planes will be treated separately. In each plane the proposed IOC has four degrees-of-freedom, namely, rigid-body translation, rigid-body rotation, and one bending mode for each cantilever beam. Thus, the corresponding admissible functions are

$$\psi_1(P) = 1 \tag{2.21a}$$

$$\psi_2(P) = \bar{z} \tag{2.21b}$$

$$\psi_3(P) = \bar{z}^2 - \bar{z}^3/3 \tag{2.21c}$$

$$\psi_4(P) = \bar{y}^2 - \bar{y}^3/3 \tag{2.21d}$$

where $\bar{z} = z/\ell_k$ and $\bar{y} = y/\ell_s$ in which ℓ_k and ℓ_s are the length of the keel (296 ft) and solar boom (132 ft), respectively.

2.5 Modal analysis of IOC model

Based on Eq. (2.21) the mass and stiffness matrices for the model are formulated in Appendices A and B. The matrix equation of free motion of the IOC is

$$\begin{bmatrix} m_{11} & m_{12} & m_{13} & m_{14} \\ m_{21} & m_{22} & m_{23} & m_{24} \\ m_{31} & m_{32} & m_{33} & m_{34} \\ m_{41} & m_{42} & m_{43} & m_{44} \end{bmatrix} \begin{bmatrix} \ddot{q}_1 \\ \ddot{q}_2 \\ \ddot{q}_3 \\ \ddot{q}_4 \end{bmatrix} + \begin{bmatrix} 0 & 0 & 0 & 0 \\ 0 & k_{22} & 0 & 0 \\ 0 & 0 & k_{33} & 0 \\ 0 & 0 & 0 & k_{44} \end{bmatrix} \begin{bmatrix} q_1 \\ q_2 \\ q_3 \\ q_4 \end{bmatrix} = \begin{bmatrix} 0 \\ 0 \\ 0 \\ 0 \end{bmatrix} \tag{2.22}$$

One may eliminate the rigid-body translation q_1 from the system by solving q_1 in terms of the rest of q's from the first equation of Eq. (2.22) and substituting it into the remaining equations. A further simplification can be made by disregarding the small coupling effect of the rigid-body rotation q_2 and the elastic modes q_3 and q_4 due to gravity gradient torque. Thus, one may eliminate both q_1 and q_2 from the system and obtain the following:

$$\begin{bmatrix} q_1 \\ q_2 \end{bmatrix} = [T] \begin{bmatrix} q_3 \\ q_4 \end{bmatrix} \tag{2.23}$$

$$\begin{bmatrix} m_{33} & m_{34} \\ m_{43} & m_{44} \end{bmatrix} \begin{bmatrix} \ddot{q}_3 \\ \ddot{q}_4 \end{bmatrix} + \begin{bmatrix} k_{33} & 0 \\ 0 & k_{44} \end{bmatrix} \begin{bmatrix} q_3 \\ q_4 \end{bmatrix} = \begin{bmatrix} 0 \\ 0 \end{bmatrix} \tag{2.24}$$

where

$$[T] = -\begin{bmatrix} m_{11} & m_{12} \\ m_{21} & m_{22} \end{bmatrix}^{-1} \begin{bmatrix} m_{13} & m_{14} \\ m_{23} & m_{24} \end{bmatrix}$$

$$\begin{bmatrix} \bar{m}_{33} & \bar{m}_{34} \\ \bar{m}_{43} & \bar{m}_{44} \end{bmatrix} = \begin{bmatrix} m_{33} & m_{34} \\ m_{43} & m_{44} \end{bmatrix} + \begin{bmatrix} m_{31} & m_{32} \\ m_{41} & m_{42} \end{bmatrix} [T]$$

The two elastic frequencies of the IOC can be written out directly in the form

$$\omega_{1,2}^2 = \frac{\bar{m}_{33}\, k_{44} + \bar{m}_{44}\, k_{33} \mp \sqrt{(\bar{m}_{33}\, k_{44} - \bar{m}_{44}\, k_{33})^2 + 4\bar{m}_{34}\, \bar{m}_{43}\, k_{33}\, k_{44}}}{2(\bar{m}_{33}\, \bar{m}_{44} - \bar{m}_{34}\, \bar{m}_{43})} \tag{2.25}$$

and the eigenvector is

$$\{\phi_i\} = \begin{bmatrix} T_{11}(\bar{m}_{34}\, \omega_i^2) + T_{12}(k_{33} - \bar{m}_{33}\, \omega_i^2) \\ T_{21}(\bar{m}_{34}\, \omega_i^2) + T_{22}(k_{33} - \bar{m}_{33}\, \omega_i^2) \\ \bar{m}_{33}\, \omega_i^2 \\ k_{33} - \bar{m}_{33}\, \omega_i^2 \end{bmatrix} \quad i = 1,2 \tag{2.26}$$

2.6 Rigid-body librational motion of IOC

The equations of librational motion of an orbiting body which has its principal axes parallel to the orbital axes subjected to disturbing torque M can be written directly in the form [3]

$$I_x\ddot{\theta}_x + 3\,\omega_o^2(I_y - I_z)\theta_x = M_x \tag{2.27}$$

$$I_y\ddot{\theta}_y + 3\,\omega_o^2(I_x - I_z)\theta_y = M_y \tag{2.28}$$

where the I's are the moments of inertia about their respective principal axes through the center of mass. The orbital frequency of a circular orbit is

$$\omega_o = \sqrt{\mu/R^3} \quad \text{rad./s} \tag{2.29}$$

where R is the orbital radius and the gravitational constant

$$\mu = 1.407 \times 10^{16}\ \text{ft}^3/\text{s}^2$$

$$= 3.986 \times 10^{14}\ \text{m}^3/\text{s}^2$$

Thus, Eqs. (2.27) and (2.28) yield the librational frequencies

$$\omega_x = \omega_o \sqrt{3(I_y - I_z)/I_x} \tag{2.30a}$$

$$\omega_y = \omega_o \sqrt{3(I_x - I_z)/I_y} \tag{2.30b}$$

2.7 Response of IOC to crew motion due to rigid-body modes

As shown in Figure 6, due to the arrangement of the modules, crew motion will create a disturbing force either in x-direction (motion in horizontal modules) or z-direction (motion in vertical modules). Hence, the torque M_x is negligible in comparison with M_y which has the magnitudes,

$$M_y = \begin{cases} f_x Z_a & \text{(motion in horizontal modules)} \\ f_z X_a & \text{(motion in vertical modules)} \end{cases} \tag{2.31}$$

As indicated by Eq. (2.30), the librational frequency is approximately equal to $\sqrt{3}$ times the orbital frequency ($I_x \cong I_y$, $I_z << I_x$, see Table 1). The crew kicking motion is completed in a time interval of 1 second which is very short in comparison with the period of librational motion of 3,300 second. This means that the torque can be treated as an impulse torque. The action of an impulse torque is equivalent to give the space station an initial angular velocity, i.e.,

$$\hat{M}_y = \int_o^t M_y(t)dt = \dot{\theta}_y(0)\, I_y \tag{2.32}$$

The solution of Eq. (2.28b) is simply

$$\theta_y = (\hat{M}_y/\omega_y)\sin\omega_y t \tag{2.33}$$

Using the mathematical model for crew motion given by Eq. (2.16), one obtains the response at P_e

$$u(P_e,t) = Z_e\theta_y$$

$$= \begin{cases} \frac{1}{2} Z_e Z_a f_o t_1/\omega_y I_y)\sin\omega_y t & \text{(motion in horizontal module)} \\ \frac{1}{2} Z_e X_a f_o t_1/\omega_y I_y)\sin\omega_y t & \text{(motion in vertical module)} \end{cases} \tag{2.34}$$

The magnitude of acceleration produced by crew motion at P_e is

$$a(P_e) = \begin{cases} Z_e Z_a f_o \omega_y t_1/2I_y & \text{(motion in horizontal module)} \\ Z_e X_a f_o \omega_y t_1/2I_y & \text{(motion in vertical module)} \end{cases} \tag{2.35}$$

3. Numerical Results of Acceleration Due to Crew Motion

Using data given in Table 4.3.3.4-2 to 4.3.3.4-4 of Reference 1, Table 3 is formed for the formulation of the mass matrix for IOC space station. Note that the total weight given by Tables 4.3.3.4-2 and 4.3.3.4-4 [1] is 77,600 lbs heavier than that given by Table 2. In an effort to match the total weight given in Table 2, some of the weights are not included. There is a significant difference on the location of the center of mass between the present model to that given in Table 2, as shown in the following:

	Table 2	Present Model	Difference
With Orbiter	68.3 ft	113.8 ft	14.4 ft
Without Orbiter	128.2	59.5	8.8

Consider that the distance from the reference point to the microgravity experiment is equal that of the location of crew motion, i.e., $z_e = z_c = -55$ ft. The magnitude of acceleration on the microgravity experiment due to crew motion as given by Eq. (2.20b) is

$$a_e = [\phi_{1j} + \phi_{2j}(z_e/\ell_k)]^2 (f_o/M_{jj}\omega_j t_1) [A_j(t)]_{max} \quad j = 1,2 \qquad (3.1)$$

The value of $[A_j(t)]_{max}$ can be estimated from curves given in Figure 4 for a given value of ω. The summation is omitted so that a_e is calculated for each mode. Based on the librational motion approach, one has from Eq. (2.35)

$$a_e = Z_e{}^2 f_o \omega_y t_1 / 2I_y \qquad (3.2)$$

The numerical resulted obtained are summarized in Table 4.

It is important to note the following:

(1) No direct comparison can be made on the frequencies obtained to that given in Table 4.3.3.3-3 [1] due to the difference of inertia properties of the models, and furthermore, the JSC model has no distinct fundamental mode that can be singled out.

(2) The acceleration level obtained here is about one order smaller than that given by Table 4.3.3.5-15 [1]. This is due to the fact that the inertia data given by Table 4.3.3.5-6 [1] is about 1/3 of that given by Table 4.3.3.5-6 [1] (without orbiter). In addition, the disturbance torque given by Table 4.3.3.5-7 [1] is more than 2 times the value used here. Thus, the magnitude of accelerations presented in Table 5 are reasonable.

(3) Motion of the space station in Y-Z plane will occur if the disturbing force is in the direction parallel to the solar boom.

(4) The acceleration given by the librational motion is 10^{-3} of that given by elastic motion. This, due to the frequency of librational motion, is only 10^{-3} of the frequency of elastic motion.

4. Design Characteristics of Suspension System

4.1 Acceleration response of a vibration absorber system

Consider that a microgravity experiment package is mounted on the laboratory module structure which has motion $u_o(t)$ as a result of crew motion or other disturbance. As shown in Figure 3, $u_o(t)$ is approximately a harmonic. It is required to design a suspension system which can effectively reduce this disturbance over some frequency range. Vibration can be effectively reduced by using a vibration absorber [4] which is a mass-spring-damper system attached to the main mass-spring system as shown in Figure 7.

Denoting u_o, u_1, u_2, the absolute displacement of the structure, main mass, and absorber mass, respectively, the equations of motion of the system are

$$m_1\ddot{u}_1 + c\dot{u}_1 + (k_1 + k_2)u_1 - c\dot{u}_2 - k_2u_2 = k_1u_o(t) \tag{4.1a}$$

$$m_2\ddot{u}_2 + c\dot{u}_2 + k_2u_2 - c\dot{u}_1 - k_2u_1 = 0 \tag{4.1b}$$

Letting the input $u_o(t)$ be a harmonic disturbance, one may put

$$u_o(t) = U_o e^{i\omega t} \quad , \quad u_1 = U_1 e^{i\omega t} \quad , \quad \text{and} \quad u_2 = U_2 e^{i\omega t} \quad i = \sqrt{-1} \tag{4.2}$$

where U_1 and U_2 are complex quantities that can be determined from the matric equation

$$\begin{bmatrix} (k_1 + k_2 - m_1\omega^2 + ic\omega) & -(k_2 + ic\omega) \\ -(k_2 + ic\omega) & (k_2 - m_2\omega^2 + ic\omega) \end{bmatrix} \begin{bmatrix} U_1 \\ U_2 \end{bmatrix} = \begin{bmatrix} k_1U_o \\ 0 \end{bmatrix} \tag{4.3}$$

If one wishes to determine acceleration response rather than displacement, set

$$\ddot{u}_1 = A_1 e^{i\omega t} \quad \text{with} \quad A_1 = -\omega^2 B_1 \tag{4.4}$$

Now, let M_a denote the magnification factor of acceleration, the ratio of A_1 to input acceleration,

$$M_a = |A_1| / U_o \omega^2 \tag{4.5}$$

First, introduce the following dimensionless parameters:

$$k = k_1/k_2 \quad \mu = m_2/m_1 \quad \zeta = c/2\sqrt{m_2 k_2} \quad r = \omega/\omega_n \tag{4.6}$$

It can be shown that

$$M_a = \left\{ [(1 - \mu k r^2)^2 + 4\mu k \zeta^2 r^2] / D \right\}^{1/2} \tag{4.7}$$

where

$$D = \left\{ 1 - [1 + (1+k)\mu] r^2 + \mu k r^2 \right\}^2 + 4\mu k \zeta^2 r^2 \, [1 + (1+\mu) r^2]^2$$

4.2 Design considerations

The magnitude of the magnification factor of acceleration depends on four parameters:

k, the spring ratio (main spring/absorber spring),

μ, the mass ratio (absorber mass/main mass),

ζ, damping factor (damping coefficient/critical damping),

r, frequency ratio (space station frequency/natural frequency of main mass-spring system).

To plot M_a versus frequency ratio squared as shown in Figure 8, six sets of curves are illustrated for $\zeta = 0.2$. The first three sets are for fixed values of $\mu = 0.01$, 0.025, and 0.05, respectively, with various values of k. The next three sets are for fixed values of k = 10, 15, and 20, respectively, with various values of μ. All these curves have one common characteristic, M_a which can be effectively reduced for $r^2 > 2$. Since the frequency of the IOC space station in elastic vibration is about 1 rad/s, it requires that $k_1 > 2W_1/g$. For a microgravity experiment package of 1,000 lbs, the spring constant of the suspension must be less than 5 lb/in. For the frequency range $0.5 < r^2 < 2$, M_a can be made less than 0.5 by a proper combination of μ and k.

5. Conclusions

A simple structural model for simulation of IOC space station has been presented and formulation of this simple model provides engineers a simple and direct method for computing the fundamental frequencies of the space station and determining the magnitude of acceleration at any point produced by crew motion. Acceleration response of a mass-spring-absorber system to a moving support is also formulated. Design engineers can use plots of acceleration magnification factor versus frequency ratio squared to determine design parameters for the suspension system of the microgravity experiment package.

The following are some significant findings:

(1) The acceleration due to librational rigid-body motion is 3 orders smaller than that due to elastic bending motion.

(2) The frequency of librational motion is 1.8×10^{-3} rad/s, which is approximately $\sqrt{3}$ times the orbital frequency.

(3) The frequencies of elastic motion of the simple model are in the range 0.6 to 1.5 rad/s.

(4) Only the fundamental bending mode has dominant contribution to the acceleration, therefore, a simple model is adequate.

(5) An effective suspension system can reduce the acceleration to 1/4 of its magnitude, at most.

(6) The ideal location of the microgravity lab does not have to be near the center of mass of the space station.

(7) The most effective means to eliminate acceleration is to have the experiment module near the nodal point of the fundamental bending mode, as illustrated in Figure 9. This means that the factor $(\phi_{11} + \phi_{21}\, z_e/\ell_k)$ in Eq. (4.1) becomes very small. Example: The IOC without orbiter has moved the lab module 59.9 ft further away from the center of mass, but the acceleration is reduced 3 orders smaller than the IOC with orbiter.

(8) It is favorable to perform the microgravity experiments when the orbiter is not present.

(9) It is possible that by rearranging some massive elements, a minimum value of $(\phi_{11} + \phi_{21}\, z_e/\ell_k)/M_{11}$ can be reached. However, this has to be done by trial and error method.

Appendix A. Formulation of Mass Matrix

Notations:

I_{ox}, I_{oy}	moment of inertia of orbiter about x- and y-axis through C.M. of orbiter, respectively
I_{sx}, I_{sy}	moment of inertia of solar arrays about x- and y-axis through solar boom at the attachment, respectively
I_{UB}	moment of inertia of upper boom about x-axis through end of keel
I_{LB}	moment of inertia of lower boom about x-axis through attachment
ℓ_k	length of keel frame
ℓ_s	length of solar boom
M_k	mass of keel frame alone
m_k	kth concentrated mass attached to keel at distance z_k
M_s	mass of solar boom frame alone
m_s	sth concentrated mass attached to solar boom at y_s
m_r	rth concentrated mass attached to rigid main body at z_r
m_o	mass of orbiter
u_x, u_y	displacement in x and y direction respectively
$\bar{y}_s$	$= y_s/\ell_s$, coordinate of concentrated mass attached to solar boom
$\bar{z}_k$	$= z_k/\ell_k$, coordinate of concentrated mass attached to keel
z_o	coordinate of orbiter

subscripts &
summation index k(keel), r(rigid main body), s(solar boom)

A-1. Motion of IOC in X-Z Plane

The kinetic energy of rigid main body is

$$T_R = 1/2 \sum_r m_r \dot{u}_x^2(z_r)$$

$$= 1/2 \sum_r m_r[\psi_1(z_r)\dot{q}_1 + \psi_2(z_r)\dot{q}_2]^2 + 1/2\ I_{oy}[\psi_2'(z_o)\ \dot{q}_2]^2 \qquad \text{(A-1)}$$

The kinetic energy of keel structure is

$$T_K = 1/2 \sum_k m_k[\psi_1(z_k)\dot{q}_1 + \psi_2(z_k)\dot{q}_2 + \psi_3(z_k)\dot{q}_3]^2$$

$$+ 1/2\ M_k \int [\psi_1\dot{q}_1 + \psi_2(z)\dot{q}_2 + \psi_3(z)\dot{q}_3]^2\ dz/\ell_k$$

$$+ 1/2 \sum_s I_{sy}[\psi_2(z_s)\dot{q}_2 + \psi_3'(z_s)\dot{q}_3]^2 \qquad \text{(A-2)}$$

The kinetic energy of solar boom is

$$T_S = 1/2\ M_s \int [\psi_1(z_s)\dot{q}_1 + \psi_2(z_s)\dot{q}_2 + \psi_4(y_s)\dot{q}_4]^2 dy_s/\ell_s$$

$$+ 1/2 \sum_s m_s[\psi_1(z_s)\dot{q}_1 + \psi_2(z_s)\dot{q}_2 + \psi_4(y_s)\dot{q}_4]^2$$

$$+ 1/2 \sum_s I_{sx}[\psi_4'(y_s)\dot{q}_4]^2 \qquad \text{(A-3)}$$

By using Eq. (2.5) the elements of the mass matrix are obtained as follows:

$$m_{11} = M_{total} = M_r + M_k + \sum_k m_k + M_s + \sum_s m_s$$

$$m_{12} = \sum_r m_r\bar{z}_r + 1/2\ M_k + \sum_k m_k\bar{z}_k + (M_s + \sum_s m_s)\bar{z}_s$$

$$m_{13} = 1/4\ M_k + \sum_k m_k(\bar{z}_k^2 - 1/3\ \bar{z}_k^3) + (M_s + \sum_s m_s)(\bar{z}_s^2 - 1/3\ \bar{z}_s^3)$$

$$m_{14} = 1/4\ M_s + \sum_s m_s(y_s^2 - 1/3\ y_s^3)$$

$$m_{22} = \sum_r m_r\bar{z}_r^2 + 1/3\ M_k + \sum_k m_k\bar{z}_k^2 + (M_s + \sum_s m_s)\bar{z}_s^2 + \sum_s I_{sy}/\ell_k^2 + I_{oy}(\psi_2')^2$$

$$m_{23} = \frac{11}{60} M_k + \sum_k m_k\bar{z}_k^3(1 - 1/3\ \bar{z}_k) + (M_s + \sum_s m_s)(1 - 1/3\ \bar{z}_s)\ \bar{z}_s^3$$

$$+ (\sum_s I_{sy})\ \bar{z}_s(2 - \bar{z}_s)/\ell_k^2$$

$$m_{24} = \bar{z}_s m_{14}$$

$$m_{34} = (\bar{z}_s^2 - 1/3\ \bar{z}_s^3)\ m_{14}$$

$$m_{33} = (11/105)M_k + \sum_k m_k(\bar{z}_k^2 - 1/3\ \bar{z}_k^3)^2 + (M_s + \sum_s m_s)(\bar{z}_s^2 - 1/3\ \bar{z}_s^3)^2$$

$$+ (\sum_s I_{sy})\ (2\bar{z}_s - \bar{z}_s^2)^2/\ell_k^2$$

$$m_{44} = (11/105)M_s + \sum_s m_s(\bar{y}_s^2 - 1/3\ \bar{y}_s^3)^2 + 4I_{sx}\{[\bar{y}_{s1}(2 - y_{s1})^2$$

$$+ [\bar{y}_{s2}(2 - y_{s2})^2\}/\ell_s^2$$

A-2. Motion in Y-Z Plane

The kinetic energy of rigid main body is

$$T_R = 1/2 \sum_r m_r[\psi_1(z_r)\dot{q}_1 + \psi_2(z_r)\dot{q}_2]^2 + 1/2\ I_{ox}[\psi_2'(z_o)\dot{q}_2]^2$$

$$+ 1/2\ I_{UB}[\psi_2'(z_{UB})\dot{q}_2]^2 \qquad \text{(A-4)}$$

The kinetic energy of the keel structure is

$$T_K = 1/2 \sum_k m_k[\psi_1\dot{q}_1 + \psi_2(z_k)\dot{q}_2 + \psi_3(z_k)\dot{q}_3]^2$$

$$+ 1/2\ M_k \int_k [\psi_1\dot{q}_1 + \psi_2(z_k)\dot{q}_2 + \psi_3(z_k)\dot{q}_3]^2 dz_k/\ell_k$$

$$+ 1/2\ I_{UB}[\psi_2'(z_s)\dot{q}_2 + \psi_3'(z_s)\dot{q}_2]^2 \qquad \text{(A-5)}$$

The kinetic energy of the solar boom structure is

$$T_S = 1/2\ M_s \int_s [\psi_1\dot{q}_1 + \psi_2(z_s)\dot{q}_2 + \psi_3(z_s)\dot{q}_3]^2 dy_s/\ell_s$$

$$+ 1/2\ M_s \int_s \{[\psi_2'\dot{q}_2 + \psi_3'(z_s)\dot{q}_3]y_s - \psi_4(y_s)\dot{q}_4\}^2 dy_s/\ell_s$$

$$+ 1/2 \sum_s \{m_s[\psi_1\dot{q}_1 + \psi_2(z_s)\dot{q}_2 + \psi_3(z_s)\dot{q}_3]^2$$

$$+ [\psi_2'\dot{q}_2 + \psi_3'(z_s)\dot{q}_3]y_s - \psi_4(y_s)\dot{q}_4]^2\}$$

$$+ 1/2 \sum_s I_{sx}[\psi_2'\dot{q}_2 + \psi_3'(z_s)\dot{q}_3 - \psi_4'(y_s)\dot{q}_4]^2 \qquad \text{(A-6)}$$

Applying Eq. (2.5) results in the mass matrix for motion in Y-Z plane:

$$m_{11} = M_T = (m_{11})_{xz}$$

$$m_{12} = (m_{12})_{xz}$$

$$m_{13} = (m_{13})_{xz}$$

$$m_{14} = 0$$

$$m_{22}=(m_{22})_{x\bar{z}} + (\psi_2')^2 \left[\sum_s (I_{sx} - I_{sy}) + 1/3\ M_s \ell_s^2 + \sum_s m_s y_s^2 + I_{ox} - I_{oy} + I_{UB} + I_{LB}\right]$$

$$m_{23} = (m_{23})_{xz} + \psi_2'\psi_3'(z_s)\left[\sum_s (_{sx} - I_{sy}) + \sum_s m_s y_s^2 + 1/3\ M_s \ell_s^2\right] + I_{UB}\psi_2'\psi_3'(\ell_k)$$

$$m_{24} = -\left[\frac{13}{30} M_s \ell_s + \sum_s m_s y_s \psi_4(y_s) + \sum_s I_{sx}\psi_4'(y_s)\right]\psi_2'$$

$$m_{33} = (m_{33})_{xz} + \left[\sum_s m_s y_s^2 + \sum_s (I_{sx} - I_{sy})\right][\psi_3'(z_s)]^2 + I_{UB}[\psi_3'(\ell_k)]^2$$

$$m_{34} = -\left[\frac{13}{30} M_s \ell_s + \sum_s m_s \psi_4(y_s) y_s + \sum_s I_{sx}\psi_4'(y_s)\right]\psi_3'(z_s)$$

$$m_{44} = (m_{44})xz$$

The subscript "xz" denotes element of mass matrix of motion in X-Z plane.

A-3. Mass and inertia properties for IOC model

Table 3 is formed based on data given by Table 4.3.3.4-2 to 4.3.3.4-4 [1] for the purpose of formulation of the mass matrix.

Appendix B. Determination of Stiffness Matrix

B-1. Bending strain energy

The bending strain energy of keel and solar boom structure is given by

$$V = 1/2 \int_0^{\ell_k} (EI)_k[\psi_3'' q_3]^2 dz_k + 1/2 \int_0^{\ell_s} (EI)_s[\psi_4''(y_s) q_4]^2 dy_s$$

Applying Eq. (2.6), one obtains the following non-zero elements of the stiffness matrix

$$k_{33} = 4(EI)_k/3\ell_k^3 \qquad k_{44} = 4(EI)_s/3\ell_s^3$$

B-2. Moment due to gravity gradient

Using the formula given by Reference 3, the following are obtained:

Motion in X-Z Plane

$$M_y = -3(\mu/R^3)(I_x - I_z)q_2 \quad , \qquad k_{22} = 3(\mu/R^3)(I_x - I_z)$$

Motion in Y-Z Plane

$$M_x = -3(\mu/R^3)(I_y - I_z)q_2 \quad , \qquad k_{22} = 3(\mu/R^3)(I_y - I_z)$$

where the moments of inertia are about the axes through the c.m. of the IOC space station.

Appendix C. Numerical Results

C-1. Motion in X-Z plane (IOC with orbiter attached)

$$[m] = \begin{bmatrix} 18900 & -2758 & 1096 & 171.6 \\ -2758 & 3168 & 831.9 & 96.0 \\ 1096 & 831.9 & 483.7 & 43.7 \\ 171.6 & 96.0 & 43.7 & 122.9 \end{bmatrix} \qquad \omega_1^2 = 1.0431 \qquad \omega_2^2 = 6.64$$

$$\{\phi_1\} = \begin{bmatrix} 1.1135 \\ .9546 \\ -10.118 \\ .1639 \end{bmatrix} \qquad \{\phi_2\} = \begin{bmatrix} .2770 \\ .1165 \\ -6.49 \\ -411.87 \end{bmatrix} \qquad M_{11} = 29157 \qquad M_{22} = 1488$$

C-2. Motion in X-Z plane (IOC without orbiter attached)

$$[m] = \begin{bmatrix} 11590 & 376.2 & 1096 & 171.6 \\ 376.2 & 1829.6 & 831.9 & 96.0 \\ 1096 & 831.9 & 483.7 & 43.7 \\ 171.6 & 96.0 & 43.7 & 115.2 \end{bmatrix} \qquad \omega_1^2 = 2.0243 \qquad \omega_2^2 = 7.436$$

$$\{\phi_1\} = \begin{bmatrix} .1936 \\ 1.054 \\ -2.429 \\ .1095 \end{bmatrix} \qquad \{\phi_2\} = \begin{bmatrix} .9485 \\ 4.769 \\ -8.923 \\ -17.603 \end{bmatrix} \qquad M_{11} = 191.5 \qquad M_{22} = 32169$$

C-3. Motion in Y-Z plane (IOC with orbiter attached)

$$[m] = \begin{bmatrix} 18900 & -2758 & 1096 & 0 \\ -2758 & 3298 & 872.3 & -92.5 \\ 1096 & 872.3 & 513.5 & -74.5 \\ 0 & -92.5 & -74.5 & 122.9 \end{bmatrix} \qquad \omega_1^2 = .8022 \qquad \omega_2^2 = 7.881$$

$$\{\phi_1\} = \begin{bmatrix} .3673 \\ 1.194 \\ -3.332 \\ .1674 \end{bmatrix} \qquad \{\phi_2\} = \begin{bmatrix} .3332 \\ .9829 \\ -3.274 \\ -5.779 \end{bmatrix} \qquad M_{11} = 959.8 \qquad M_{22} = 3312$$

C-4. Motion in Y-Z plane (IOC without orbiter attached)

$$[m] = \begin{bmatrix} 11590 & 369.8 & 1096 & 0 \\ 369.8 & 3298 & 872.3 & -92.5 \\ 1096 & 872.3 & 513.5 & -74.5 \\ 0 & -92.5 & -74.5 & 11 \end{bmatrix} \qquad \omega_1^2 = .4301 \qquad \omega_2^2 = 7.046$$

$$\{\phi_1\} = \begin{bmatrix} .1906 \\ .510 \\ -2.191 \\ -1.716 \end{bmatrix} \qquad \{\phi_2\} = \begin{bmatrix} .3221 \\ .5438 \\ -3.589 \\ -13.17 \end{bmatrix} \qquad M_{11} = 927.5 \qquad M_{22} = 18582$$

C-5 Computation of accelerations

Using the data given above, Eq. (3.1), and with the aid of Figure 4 for the value of $[A(t)]_{max}$, acceleration of the experiment package can be calculated. The results are shown in Table 4.

References

1. "Space Station Configuration Description," Systems Engineering Integration Space Station Program Office, L.B.J. Space Center, August, 1984.

2. Craig, R. R., Jr.: "Structural Dynamics," Wiley, 1981.

3. Kane, T. R.; Likins, P. W.; and Levinson, D. A.: "Spacecraft Dynamics," McGraw-Hill, 1983, p. 177.

4. Tong, K. N.: "Theory of Mechanical Vibrations," Wiley, 1960.

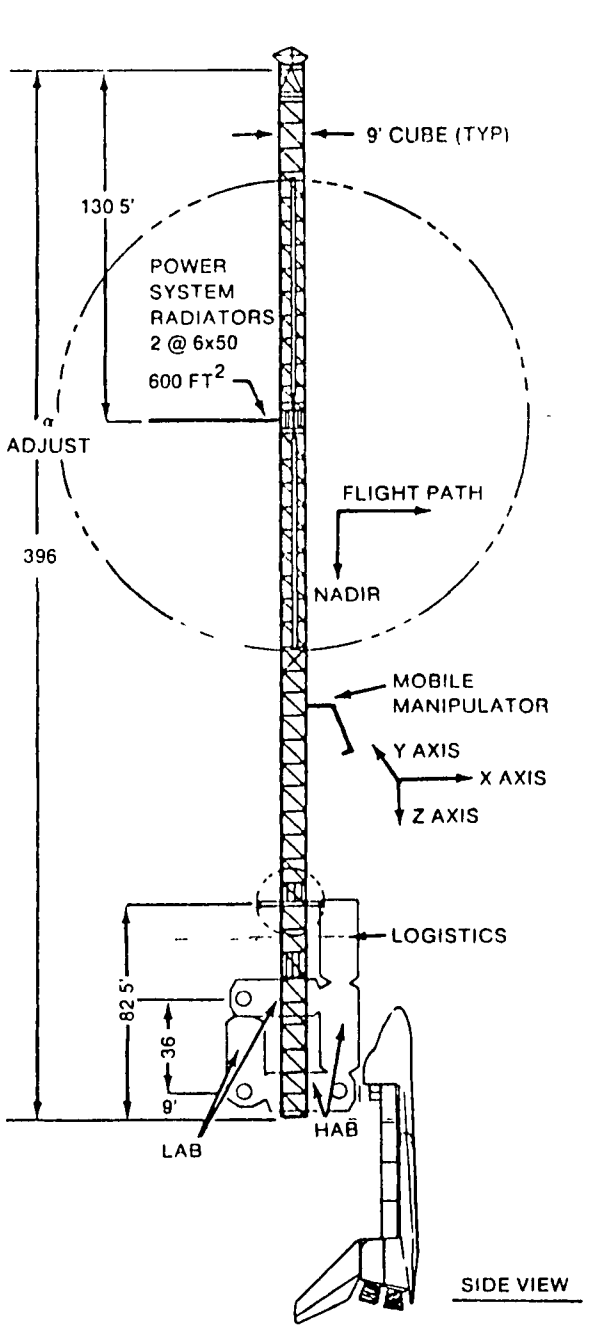

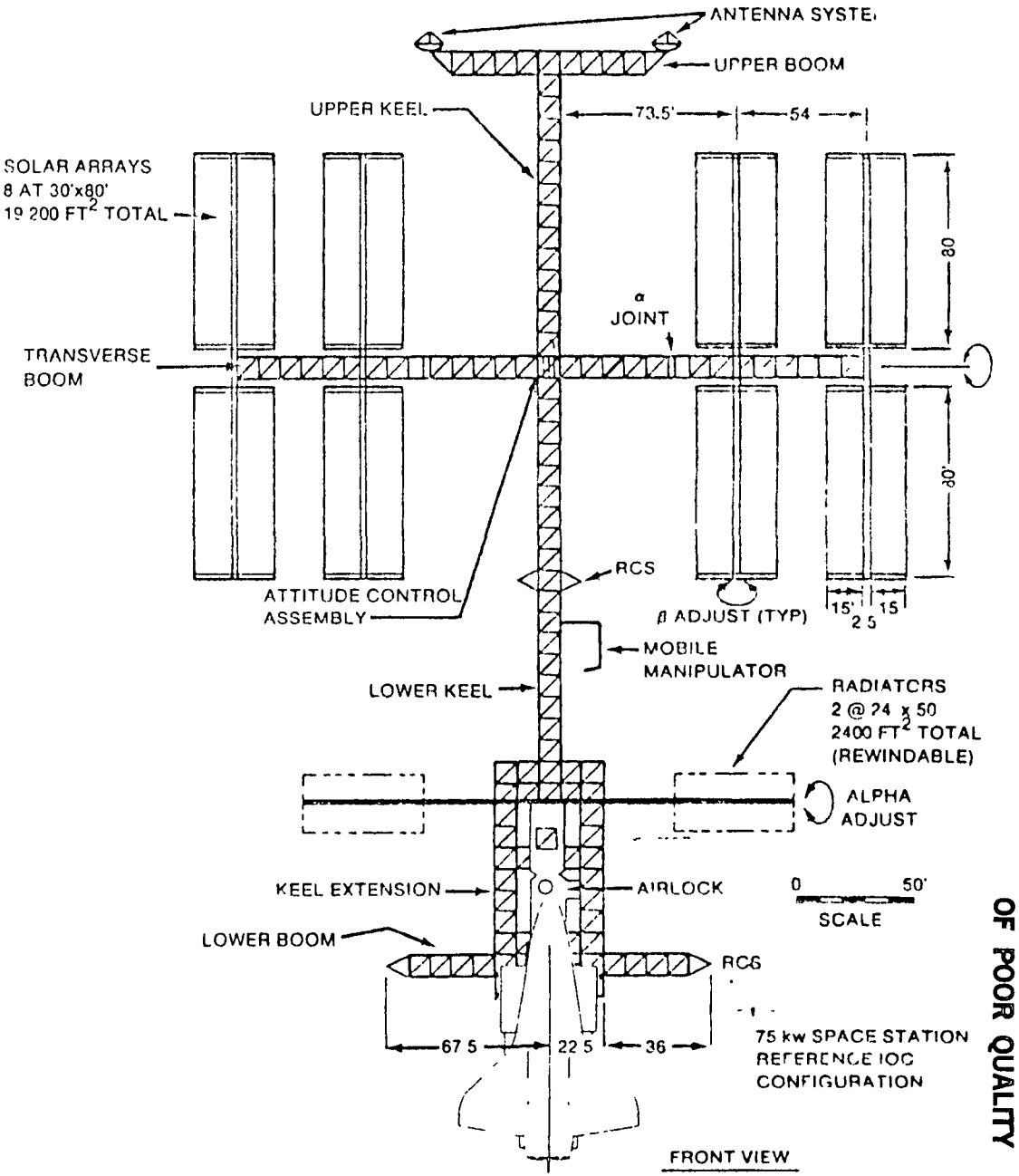

Figure 1 (Figure 4.2.1-1 [1])IOC REFERENCE CONFIGURATION

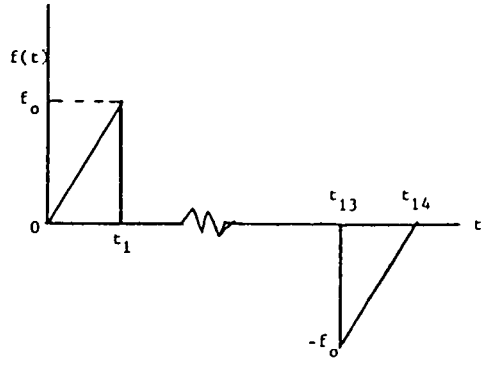

Figure 2 Mathematical Model of Crew Motion

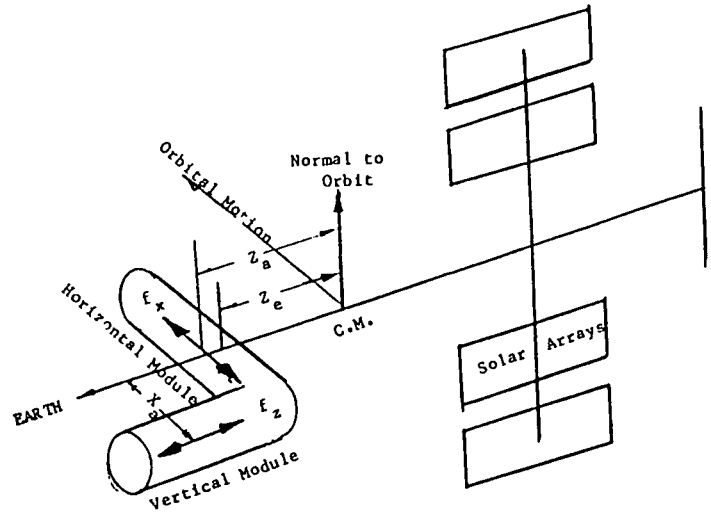

Figure 6 Reference of Crew Motion

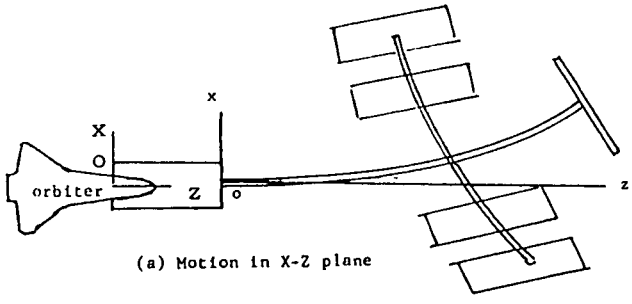

(a) Motion in X-Z plane

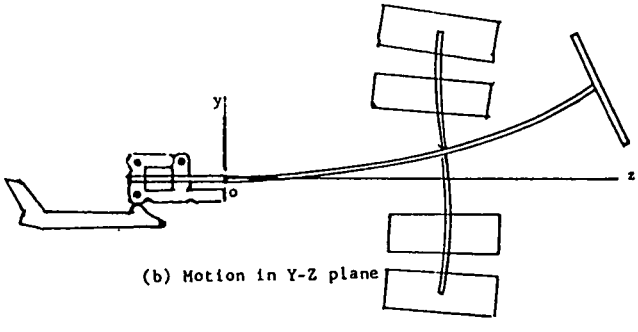

(b) Motion in Y-Z plane

Figure 5 Model of IOC Space Station

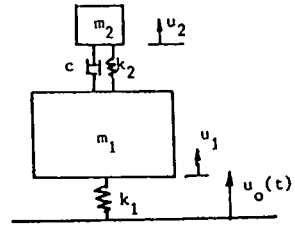

Figure 7 Model of SuspensionSystem

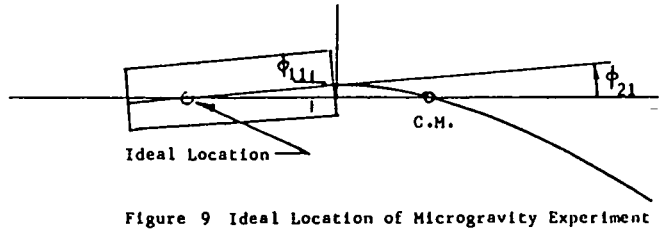

Figure 9 Ideal Location of Microgravity Experiment

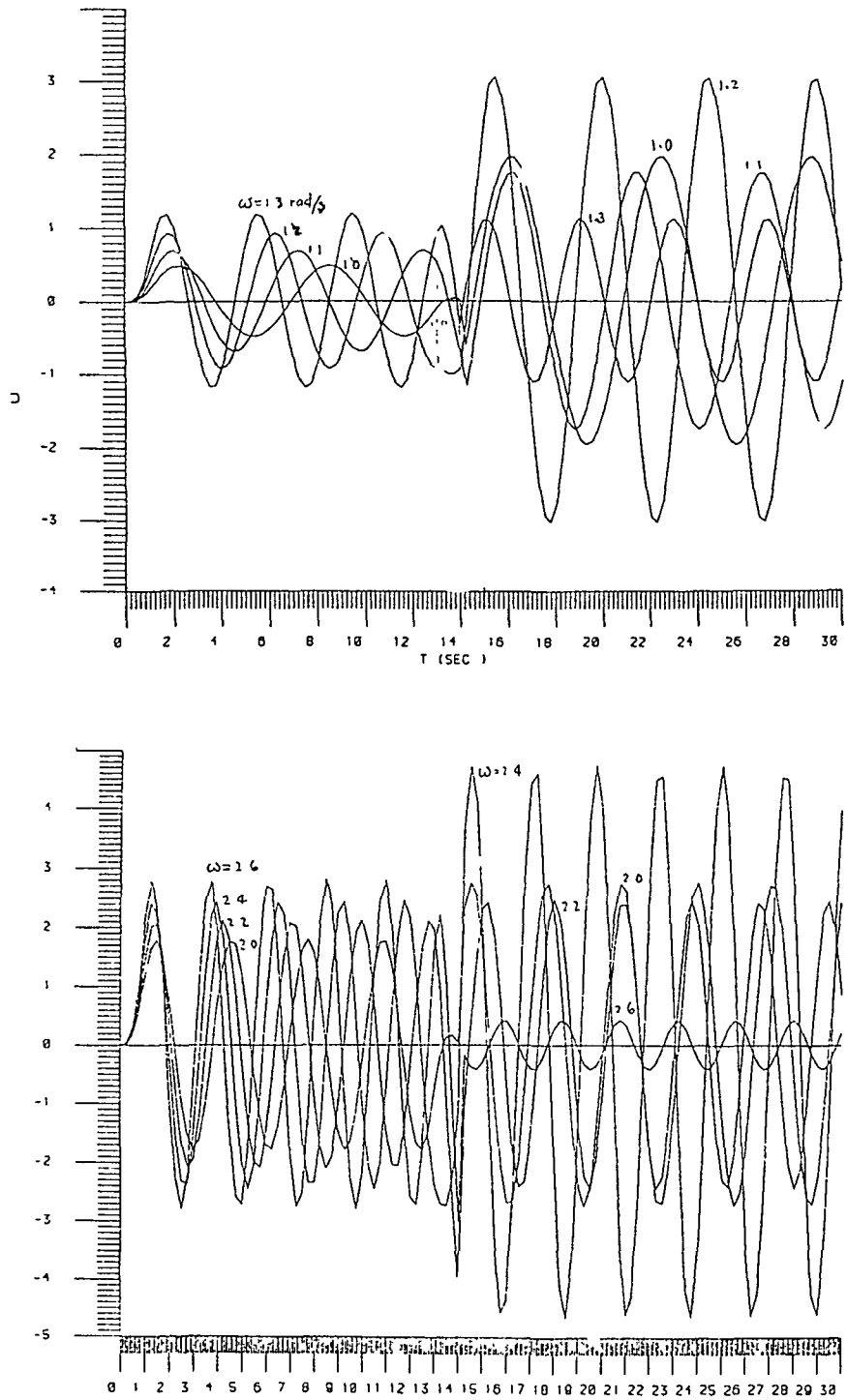

Figure 3 Displacement Functions

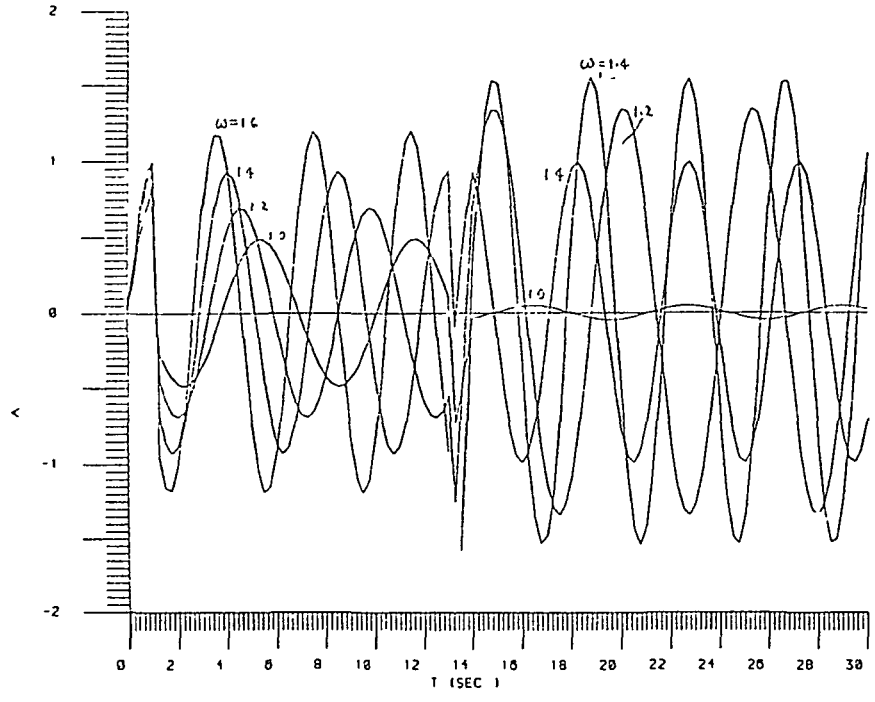

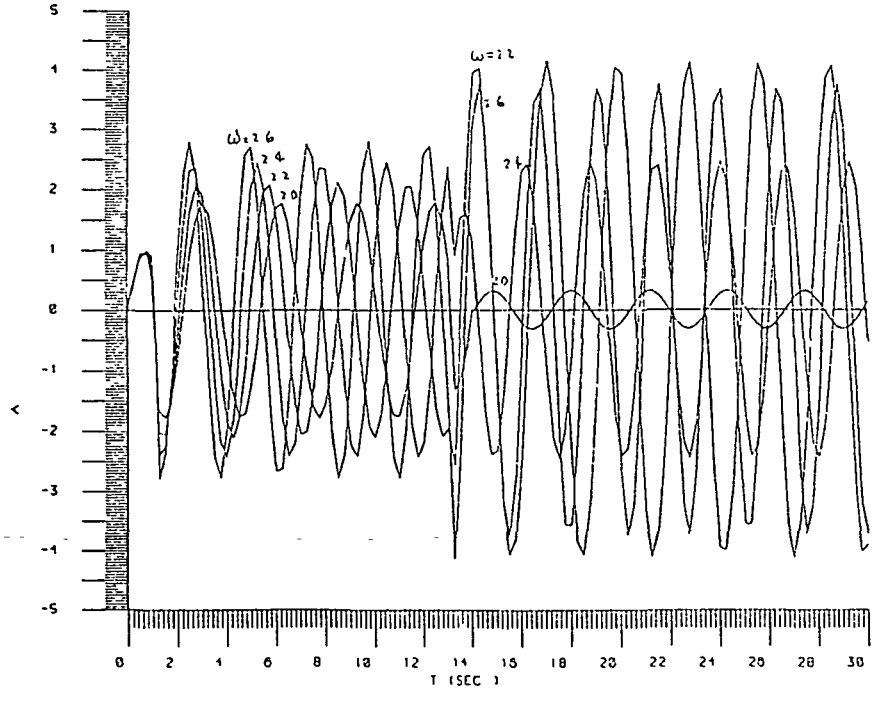

Figure 4 Acceleration Functions

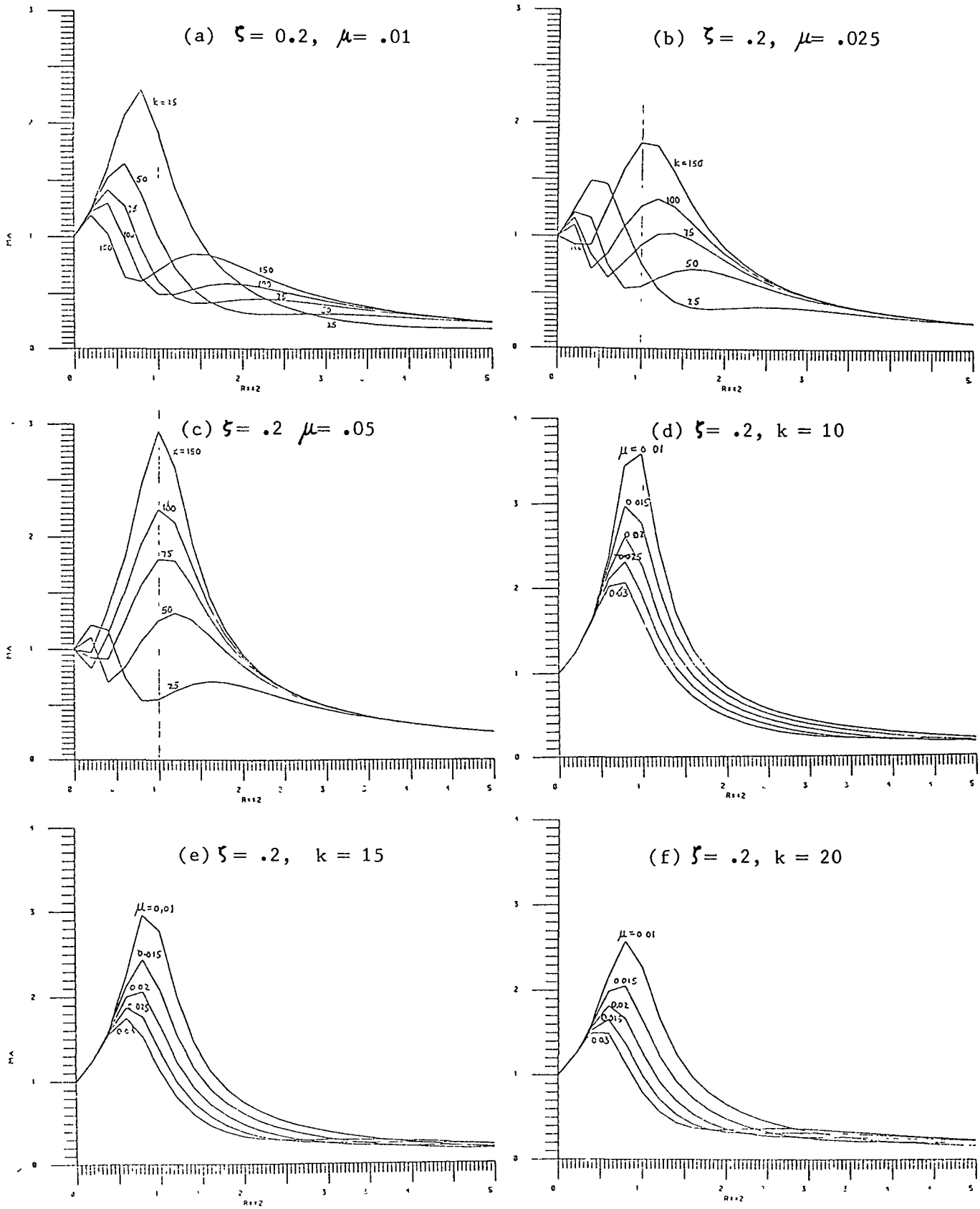

Figure 8 Acceleration Magnification Factor

Table 1. Properties of Analytical Reference Configuration Space Station Model (Table 4.3.3.3-1 [1])

Component	Bending Stiffness (ft-lbs-ft)	Torsional Stiffness (ft-lbs-ft)	Mass Length (Slugs/ft)	Bending Strength (ft-lbs)	Torsional Strength (ft-lbs)
Booms and Keels	1.31 E+9	3.18 E+8	0.25	35,000	15,000
30-Inch Astro Mast	3.13 E+6	2.08 E+5	2.3	3,480	208

Table 2. Inertial Properties of Analytical Model (Table 4.3.3.3-2 [1])

Case	Weight (lbs)	C. G. Coordinates (ft)	Moments of Inertia (lb-ft-sec^2)
Without Payloads and Orbiter	269,000	(1.1,0,84.2)	(8.63 E+7, 7.82 E+7, 1.20 E+7)
With Payloads Only	373,200	(-1.1,0,128.2)	(2.06 E+8, 1.98 E+8, 1.45 E+7)
With Orbiter Only	508,800	(5.7,0,34.4)	(1.45 E+8, 2.37 E+8, 1.35 E+7)
With Payloads and Orbiter	608,600	(3.59,0,68.3)	(3.21 E+8, 3.14 E+8, 1.62 E+7)

Table 3. Masses and Inertia Properties Used for IOC Model

r	Masses attached to main body	Z_r ft	z_r ft	W_r lbs
1	Fuel tank and gases	94.5	- 5.5	17,002
2	Module radiators	82.5	- 17.5	3,000
3	Five-bay platform	76.5	- 23.5	1,403
4	COM 1203	64.0	- 26.0	11,000
5	Logistics module	71.5	- 28.5	37,823
6	OMV and kits	67.5	- 32.5	23,750
7	Horizontal lab	45.0	- 55.0	54,295
8	Vertical lab	34.5	- 65.5	27,067
9	Keel extension	27.0	- 73.0	970
10	Vertical lab	19.5	- 80.5	47,709
11	Lower boom	13.5	- 86.5	728
12	Horizontal lab, SAA0207 and SAA0201	9.0	- 91.0	37,089
13	Orbiter	-26.66	-126.66	235,400

s	Masses attached to solar boom	Z_s ft	z_s ft	y_s ft	W_s lbs
	Solar boom structure	265.5	165.5	0-132	2,345
1	Power system radiators	265.5	165.5	54.0	750
2	TDM 2010	265.5	165.5	63.4	1,540
3	4 inboard solar arrays	265.5	165.5	78.0	4,787
4	4 outboard solar arrays	265.5	165.5	132	4,787

k	Mass attached to keel	Z_k ft	z_k ft	W_k lbs
	Upper and lower keel structure	100-396	0-296	2,504
1	Remote manipulator	162.0	62.0	2,000
2	Refuel attachment, tanks and tools	107.5	7.5	4,625
3	TDM 2570	210.5	110.5	2,000
4	Instruments and storage shelter	212.5	112.5	4,625
5	Storage boxes and tools	272.5	172.5	9.850
6	Service attachments	290.5	190.5	3,750
7	TDM 2560	295.5	195.5	7,055
8	Satellite	324.5	224.5	20,000
9	Upper boom and antenna system	396.0	296.0	17,734

Rotational Moment of Inertia	I_x ft-lb-s^2	I_y ft-lb-s^2
Orbiter (about c.m. of orbiter)	7×10^6	8×10^6
Solar array (about attachment) each		
Parallel to Nadir	101,000	107,300
Normal	2,790	107,300
Upper boom with antenna system	158,800	small
Module radiators (about attachment)	583,500	4,470
Power system radiators (about attachment)	750	25,120

Note: Z is measured from the bottom end of the keel extension and z is measured from the joint of keel and keel extension

Table 4. Numerical Results for IOC Model

Motion	ω and a_e	Motion in X-Z Plane		Motion in Y-Z Plane	
		With Orbiter	Without Orbiter	With Orbiter	Without Orbiter
Bending	ω rad/s	1.021	1.423	0.896	0.656
	a_e	$1.14\ g \times 10^{-5}$	$1.44\ g \times 10^{-8}$	$0.86\ g \times 10^{-5}$	$1.17\ g \times 10^{-5}$
	ω rad/s	2.577	2.730	2.810	2.654
	a_e	$2.26\ g \times 10^{-6}$	$1.38\ g \times 10^{-7}$	$0.66\ g \times 10^{-5}$	$2.9\ g \times 10^{-6}$
Libra. Motion	ω rad/s	1.89×10^{-3}	1.89×10^{-3}	1.85×10^{-3}	1.81×10^{-3}
	a_e	$0.254\ g \times 10^{-8}$	$5.13\ g \times 10^{-8}$	$0.24\ g \times 10^{-8}$	4.72×10^{-8}